# 2.ICSGTEIS-2021_pravat

*by* Metta Savitri

**Submission date:** 16-Apr-2023 07:58AM (UTC-0500)
**Submission ID:** 2065842749
**File name:** 2.ICSGTEIS-2021_pravat.pdf (1.26M)
**Word count:** 4316
**Character count:** 22240

# Modeling and Power Management of Electric Vehicle Charging System

Pravat Kumar Ray
*Department of Electrical Engineering*
*National Institute of Technology*
Rourkela, India
rayp@nitrkl.ac.in

Anindya Bharatee
*Department of Electrical Engineering*
*National Institute of Technology*
Rourkela, India
bharatee.anindya@gmail.com

Samarpita Panda
*Department of Electricl Engineering*
*National Institute of Technology*
Rourkela, India
117EE0378@nitrkl.ac.in

I Nyoman Wahyu Satiawan
*Department of Electrical Engineering*
*University of Mataram*
Mataram, Indonesia
nwahyus@unram.ac.id

2021 International Conference on Smart-Green Technology in Electrical and Information Systems (ICSGTEIS) | 978-1-6654-1355-8/21/$31.00 ©2021 IEEE | DOI: 10.1109/ICSGTEIS53426.2021.9650377

***Abstract*— Electric Vehicles (EVs) are gradually becoming the new normal of the automobile industry. To make Electric Vehicles a mainstream automobile there is a need to make the charging stations more accessible, sustainable, and economic. The aim of this paper is to simulate a charging station consisting of a renewable energy source (Photo Voltaic array) and a microgrid to supply power, and to study the station's power management schemes so that the microgrid experiences the least stress. The design of the station is such that the power flow occurs in both Grid to Vehicle (G2V) and Vehicle to Grid (V2G) directions. Due to this bidirectional nature of the charging station, not only is the pressure on the grids reduced but also the Electric Vehicle itself can be used to stabilize the grid during unequal production of power and load demand. The power flow in this entire system is decided by the mode of operation which depends on the load demand, microgrid production, and the State of Charge of the Electric Vehicle. The recommended power flow scheme for charging an electric vehicle is validated through MATLAB/Simulink results.**

***Keywords*— Electric Vehicle, Photo Voltaic, Grid to Vehicle, Vehicle to Grid, State of Charge**

## I. Introduction

As the dependence on conventional sources of energy decreases, the use, and popularity of renewable sources of energy for most activities increases. Likewise, with the beginning of electric vehicles, the use of conventional automobiles should reduce. However, due to high capital cost, ignorance of the masses, and the ever-developing infrastructure to accommodate electric vehicle charging, the electric vehicle industry is growing at a rather slow pace in comparison to its competitor. Currently, EV charging relies on receiving power from the existing grid and converting it to be appropriate for charging the EV batteries. However, the use of a utility grid hits the intention of employing electric vehicles. Mass EV charging will affect the smooth operation of the grid such as power fluctuations, voltage profile, increases the harmonic content due to the use of power electronics devices and nonlinear loads, and can create instability in the AC system.

Especially the charging infrastructure contributes a backup for EV to pierce today's automotive world. AC slow charging technology is one of the charging infrastructures described in [1], in which the vehicles are charged from the existing conventional grid. To charge several EVs at the same time, a DC micro-grid is essential that provides high power production and permits us to charge several EVs concurrently [2]. Compared to internal combustion engines, electric vehicles provide significant advantages. Regenerative braking allows hybrid EVs and Plug-in hybrid EVs to collect and store kinetic energy that would otherwise be lost as heat during friction braking [4]. The integration of a conventional microgrid with a PV array such that an EV can be charged and discharged without hampering the grid stability is the main focus in [16-18].

To power electric vehicles, the intelligent charging system for electric vehicles proposed in this paper mainly depends on PV power generation [14]. If the power generated from PV is insufficient, then only EVs are supplied by the microgrid. During peak demand hours EVs can go into the V2G mode of operation and supply power to the microgrid. As a result, there is a bidirectional energy flow between the EV battery and the microgrid, but power from the PV array exclusively goes towards the load. To link the EV battery, PV array, and microgrid, suitable Power electronic interfacings are used.

The key motivation of the paper is to model a small smart charging system for electric vehicles. The charging station is designed in such a way that it will reduce the stress from the utility grid. During high demand and low PV generation, the direction of power flow has been reversed that is from vehicle to grid.

The detailed architecture and control scheme for the EV charging station is explained in section II. Section III describes the EV battery system along with the structure of the DC-DC bidirectional converter. The simulated results are discussed in section IV and the paper is wound up in section V.

## II. Architecture and Control of Proposed EV Charging Station

### *A. Architecture of Smart Grid*

The charging facility is depicted in block diagram form in Fig. 1. A shared dc link, powered by the PV system or the main grid, depending on the total connected load and the amount of solar radiation accessible, enables EV charging. An AC-DC bidirectional power converter connects the utility grid to the dc bus, a boost converter in conjunction with a maximum power point tracking (MPPT) connects the PV



Authorized licensed use limited to: NATIONAL INSTITUTE OF TECHNOLOGY ROURKELA. Downloaded on April 16,2023 at 12:24:07 UTC from IEEE Xplore. Restrictions apply.

system to the dc link, and a bidirectional converter controls the charging and discharging of the EV battery [11]. The power flow direction is decided by the control logic for each of the blocks of the charging station.

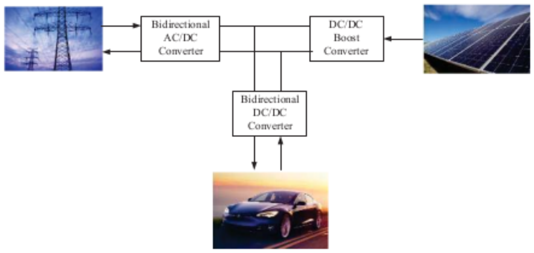


Fig. 1. Charging station block diagram.

## B. Modes of Operation

The smart EV charging station has three operation approaches that determine the direction in which electricity flows among its numerous components. The dc link voltage, the state of charge (SOC) of the electric vehicle battery, amount of power produced from the PV arrangement, and the loads connected to the utility grid play a role in how this EV charging station operates (the present loads on the utility grid can be known from the local data acquisition centre using methods described in [9]). The intermittent power flow of the PV array and the corresponding dc-link voltage fluctuations are utilized to control the whole system by monitoring and regulating the voltage level and permitting the system to operate in several modes.

*1) Charging of electric vehicle through Photovoltaic power:* In this approach, the total power available from the PV array exceeds the power required for EV charging and EV battery SOC is less than the specified $EV_{SOC}$. In this condition, the bidirectional DC-DC converter linked to the EV unit recharges the EV battery in buck mode. When the EV battery's SOC hits $EV_{SOC}$, the charging stops and the total power available from PV units are fed into the utility grid. As a result, in mode 1 functioning, there are two scenarios. In the first case, total power produced by PV is used for the EV battery charging and to feed the utility grid. In the latter case, once the EV battery crossed its predefined SOC level, the total PV production is provided to the grid and the charging of the battery has been stopped.

*2) Electric Vehicle is charged by taking power from both PV and Utility grid:* In this approach, the available PV power is inadequate to charge the EV alone. As a result, the EV battery is charged by taking power from both PV and grid. The bidirectional power converter connected to the grid operates in rectification mode, whereas the bidirectional DC-DC power converter connected to the EV battery operates in buck mode [10].

*3) Vehicle to grid mode (V2G Mode):* In this mode of operation, the EV battery SOC is greater than the specified threshold limit and the total available PV and grid power are insufficient to meet the power demand. To enhance the steadiness of the system during highest load periods, the EV battery is depleted and required power is supplied to the utility grid [10].

## C. Control of AC/DC Bidirectional Converter

In the planned architecture of the smart EV charging system, the utility grid, when connected to the common dc bus, is subjected to bidirectional power flow and therefore requires a bidirectional AC-DC power converter for power modulation. During peak load time EVs discharge and the utility grid takes power from them under the V2G mode of operation. Conversely, power is delivered by the utility grid to the common dc bus which is absorbed by EVs when required.

A rectifier circuit in conjunction with a balanced three-phase supply can be used directly to power a balanced three-phase load. As the supply has a constant amplitude and frequency, upon rectification, a fixed voltage DC power supply can be obtained. Several filters like the LCL filter are used with the rectifier circuit to reduce the ripple content on the output side.

A control algorithm based on synchronous reference theory is used to control the converter. As shown in Fig. 2, the line-to-line voltages are transformed to two-phase voltages using Park's transformation for the Phase Locked Loop (PLL) implementation. PLL produces the reference signal which is used to implement the current controller in a grid-connected inverter. The voltages are converted to d-q voltages using Clarke's transformation. A PI controller is used to make $V_q$ zero. The PI controller output is given to an integrator to find the value of new $\omega t$. Sine and cosine functions are used to generate active (in phase with $\alpha$) and reactive components (in phase with $\beta$) of the reference signal. For current controller implementation, either grid current or inverter current is used. These currents are converted to the α-β domain using Park's transformation then to the d-q domain using Clarke's transformation ($I_d$ = active current and $I_q$= reactive current). $I_d$ and $I_q$ are subtracted from their respective reference currents to find a deviation which is provided to a PI controller (current controller) to find voltages $U_d$ and $U_q$.

$$V_d = U_d + E_d + L\omega I_q \quad (1)$$

$$V_q = U_q + E_q - L\omega I_d \quad (2)$$

where $L$ is LCL filter inductance and ω is angular frequency of the grid. For the sine PWM scheme, the relation between modulation index and inverter voltage is given by

$$V_d = \frac{m_d \times V_{dc}}{2} \quad (3)$$

$$V_q = \frac{m_q \times V_{dc}}{2} \quad (4)$$

So, to get $E_q$ and $E_d$, $V_q$ and $V_d$ are be multiplied with $\frac{2}{V_{dc}}$. Then $E_q$ and $E_d$ are transformed to get the abc voltages which are further used as reference voltages for PWM generation. The PWM signal is then fed to the gate terminals of IGBTs in the inverter. This inverter is changed to work as a bidirectional converter by implementing a DC voltage loop. $V_{dc}$ must be compared to the reference $V_{dc}$ = 600V (the voltage we wish to maintain at the DC link) and fed to a PI controller whose output is a reference for d-axis current loop.



Authorized licensed use limited to: NATIONAL INSTITUTE OF TECHNOLOGY ROURKELA. Downloaded on April 16,2023 at 12:24:07 UTC from IEEE Xplore. Restrictions apply.

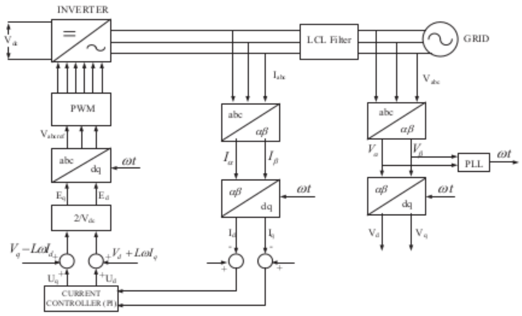


Fig. 2. Block diagram of DC-AC inverter control algorithm with theory based on Synchronous reference frame.

### D. Control Scheme Boost Converter Connected to PV array

Photovoltaics (PV) modules use solar cells accumulated into solar panels for conversion of solar energy into electricity. One of the major sources of renewable energy is the sun. It is one of the fastest-growing renewable energy harnessing technologies. The efficiency of a PV system refers to the percentage of solar energy that can be converted into electrical energy.

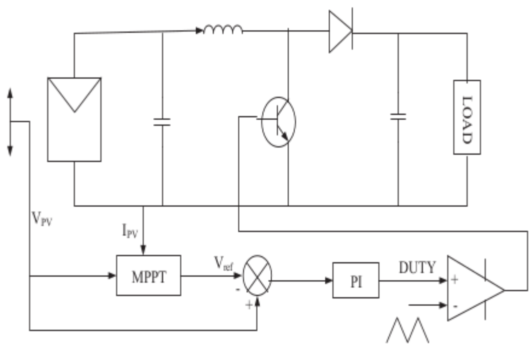


Fig. 3. Block diagram of PV array connected to boost converter with the control scheme.

A boost converter is used to step up a given DC voltage to a required level. In this case, the PV array provides a Voltage of 250V-350V, which is less than the reference DC link voltage. So, a boost converter is designed according to [5]. The control of boost converter connected to PV array is done by using MPPT algorithm which advances the overall efficacy of the PV unit [6]. The efficiency of power transfer from the PV module to the load depends on the present irradiance level and the load characteristics. MPP trackers help in changing the load characteristics to keep up with the changing irradiance level for optimal power transfer. This particular load characteristic is known as the maximum power point (MPP) and MPPT is the process of obtaining this point and maintaining the operation there. Among the various MPPT algorithms devised to date, Perturb and Observe algorithm is most frequently employed as it is simpler and fairly effective when compared with other MPPT algorithms [7]. Fig. 3 expresses the detailed control scheme of the boost converter connected to the PV array by using the MPPT technique. Voltage and current from the PV array are utilized to execute MPPT to get reference voltage as output. This reference voltage is subtracted from the actual PV voltage and the mismatch between them is then provided to a PI controller. The output produced from PI controller gives the duty ratio for PWM generation. This duty ratio is then compared with a carrier signal to give the PWM which acts as the gate signal of IGBT. This method contains a closed-loop control mechanism.

## III. Structure of EV Battery with DC/DC Bidirectional Converter

Integrating all of the separate devices and maintaining the requisite voltage across the DC bus is the difficult part of creating an EV charging station. To prevent voltage ripples over the DC bus, interfaces and converters are commonly linked to it using an inductor in series with the output and a capacitor in parallel with it. The voltage across the DC bus must be close to the prescribed value in all modes of operation. The output voltage across the DC bus is controlled in Grid-connected mode by the closed-loop control system of the three-phase AC-DC converter, as well as the closed-loop control strategy of the Battery Interface's DC-DC bidirectional converter. The PV module's control strategy is designed to provide voltage and current depending on MPPT and the irradiance and temperature conditions in a particular state. In the event of a V2G arrangement, the Battery Interface's closed-loop regulation keeps the DC bus voltage at the required level.

### A. EV Battery

An electric vehicle is represented in this paper by a battery that must be charged using a charging circuit connected to a charging station. If necessary, it may also be discharged to supply electricity back into the electrical system. In this case, an electrical model of an electric vehicle battery is used, which is reasonably realistic in terms of its features. In most cases, Lithium-Ion batteries are employed in electric vehicle applications. When compared to other options, these batteries offer a higher energy density, allowing them to have a greater capacity. They have a lesser tendency for self-discharge and require less maintenance.

A Thevenin equivalent battery model is utilized in Fig. 4, along with a series resistance $R_s$ to simulate the voltage and current characteristics and a parallel RC circuit in series with the open-circuit voltage source to assist identify the battery reaction to transients.

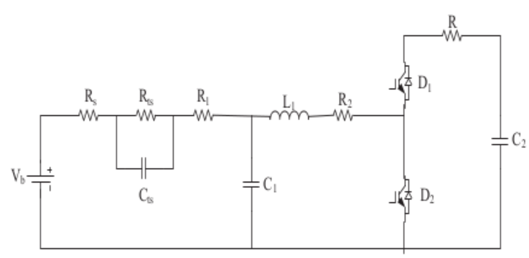


Fig. 4. Block diagram of the EV and Buck-Boost converter integration.

### B. Control Scheme for DC-DC Bidirectional Converter

The overall charging and discharging process depend on the common dc link voltage and the SOC of the battery. The employed control logic is such that, if the dc link voltage is less than 600V and the SOC of the EV battery is greater than $EV_{SOC} (= 30\%)$ of its rated value the EV battery discharges



Authorized licensed use limited to: NATIONAL INSTITUTE OF TECHNOLOGY ROURKELA. Downloaded on April 16,2023 at 12:24:07 UTC from IEEE Xplore. Restrictions apply.

and feeds power to the utility grid through the dc bus until either the voltage of the dc bus exceeds 600V or the SOC of the EV battery falls below defined $EV_{SOC}$. Similarly, the EV battery charges only if the common dc bus voltage is greater than or equal to 600V. Additional control is employed to maintain a constant charging current through the EV battery to ensure safe operation. The charging and discharging control schemes for EV battery are shown in Fig. 5.

It is a DC-DC buck-boost converter that can transmit power in both directions. It is made up of two IGBT switches. Switch D2 works in the V2G mode (discharging mode), and the converter functions as a boost converter. The duty cycle of the PWM signal to the gate of IGBT switch D2 is adjusted to raise the battery terminal voltage to slightly over 600V, allowing power to flow from the EV battery to the common dc bus. During EV charging, on the other hand, the switch D1 is on, and the converter is in buck mode. The overall charging and discharging process depend on the common dc bus voltage and the battery SOC. The EV associated to the DC-DC converter is presented in Fig. 4. The control strategy for charging and discharging of EV battery is presented in Fig. 5.

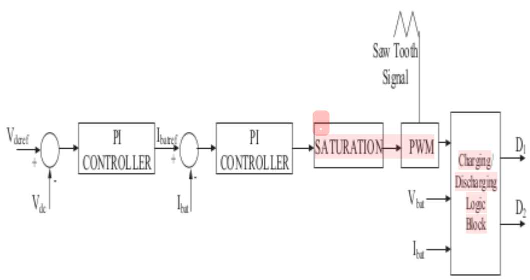


Fig. 5. Block diagram of the control scheme for Buck-Boost converter integration.

## IV. Results and Discussion

The Integrated smart EV charging station is simulated using MATLAB/Simulink and the outcomes acquired are presented in this section. The variables applied here for the simulation work are given in TABLE I.

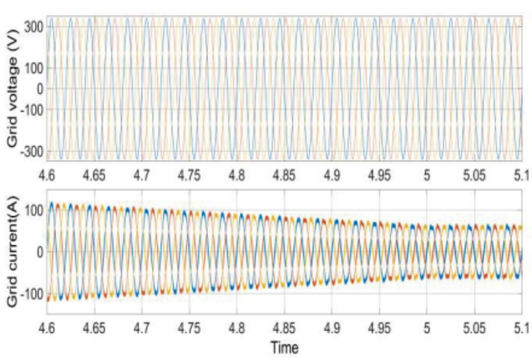


Fig. 6. Grid voltage and current when irradiance is reduced.

The grid voltage is always constant and grid current depends on the amount of PV power generation. In Fig. 6, the utility grid voltage and current are shown, where it is visible that when the PV irradiance is decreased, the grid current is reduced accordingly.

TABLE I SIMULATION PARAMETERS

| PV Array Specifications | Values |
|---|---|
| Open circuit voltage ($V_{oc}$) | 36.3V |
| Short circuit current ($I_{sc}$) | 7.84A |
| voltage at max. power ($V_{mp}$) | 29V |
| Current at max. power ($I_{mp}$) | 7.35A |
| **DC-DC Boost Converter Specifications** | **Values** |
| Switching frequency ($f_{sw}$) | 5KHz |
| Inductance ($L$) | 1.75mH |
| Capacitance ($C$) | 3227μF |
| **Battery Specifications** | **Values** |
| Nominal Voltage | 300V |
| Rated capacity | 100Ah |
| **Grid Specifications** | **Values** |
| $V_{rms}$(Ph-Ph) | 415V |
| Frequency | 50Hz |
| **LCL Filter Parameter** | **Values** |
| Inductances ($L_1, L_2$) | 500μH |
| Capacitance($C$) | 100μF |
| DC-link voltage | 600V |
| Rated load power | 10KW |

Fig. 7 shows the SOC and $I_b$ of the EV battery before the EV is integrated with the microgrid and the PV array. As seen from Fig. 7, the EV battery is adjusted to an primary SOC of 45% and at t =1sec from the start of the simulation, the EV is forced to discharge due to fluctuations from the supply that feeds the EV, so that it maintains a constant voltage of 600V across the load. As EV is not connected to any source at the starting of the simulation, battery current is oscillating. This oscillating battery current will affect the battery life. When the battery discharges, it has a negative mean value while charging changes to a positive value of discharge current. The battery would not have discharged if this fluctuation from the source side occurred simultaneously when its SOC was below 30%.

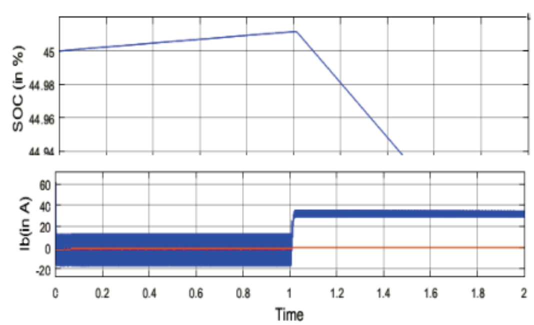


Fig. 7. SOC, Battery Voltage ($V_b$) and current flowing from battery ($I_b$) when the mode is changed from charging to discharging.



Authorized licensed use limited to: NATIONAL INSTITUTE OF TECHNOLOGY ROURKELA. Downloaded on April 16,2023 at 12:24:07 UTC from IEEE Xplore. Restrictions apply.

The Fig. 8 represents the variation of various battery parameters after it is integrated with the PV array and the microgrid common DC link. The initial SOC was set to 60% (>30%). In this mode, the PV array received an irradiance of 1kW/m2 which is the set rated value of irradiance, so the EV gets charged predominantly from the PV array. The $V_b$ is maintained at nominal voltage while the SOC of the battery increased slowly but linearly over time. A lot of oscillations were observed in the battery charging current.

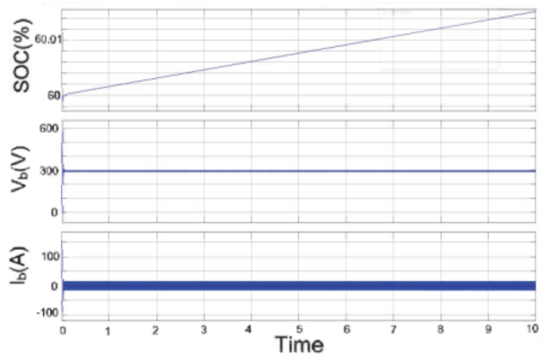


Fig. 8. SOC, $V_b$ and $I_b$ for mode-1 operation.

From Fig. 9, it was observed that the initial SOC was set to 45% (>30%). In this mode, the PV array received an irradiance less than 1000W/m2 so the PV array gets disconnected from the DC link and the microgrid becomes the main source of supply for all the connected loads and the battery. The $V_b$ is maintained at a value a little less than the nominal voltage of 300V as observed from Fig.9, while the SOC of the battery increased slowly but linearly over time. A lot of oscillations were observed in the battery charging current whose mean value was negative as can be seen from Fig. 9.

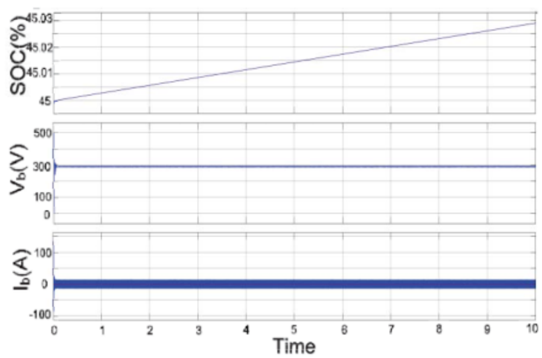


Fig. 9. SOC, $V_b$ and $I_b$ for mode-2 operation.

The initial SOC of the battery was set to 100%. The dynamic load connected to the microgrid was made to fluctuate while the PV array received a very low irradiance, the DC link voltage connected to the microgrid and PV system fell below 600V as none of the sources can supply constant power to the link. So, this led the battery to enter mode 3 of operation and it discharges from 100% as observed from Fig. 10 with the decrease in SOC. The battery voltage is almost at its peak as it is charged to 100%, and the battery current has a mean positive value as it discharges.

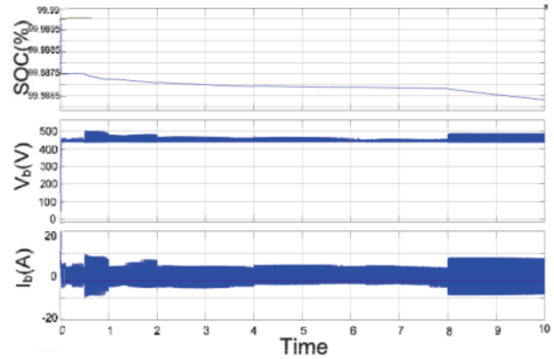


Fig. 10. SOC, $V_b$ and $I_b$ for mode-3 or V2G operation.

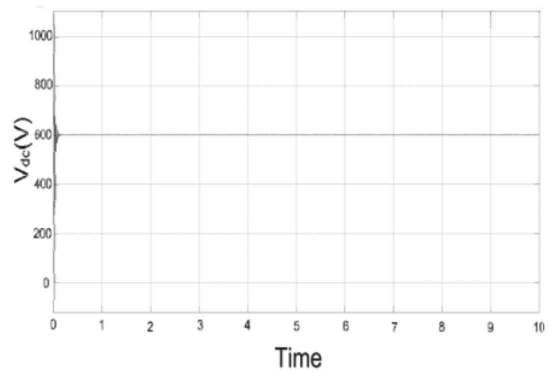


Fig. 11. DC link voltage when charging station operates in mode-3.

As seen from Fig. 11, the DC link voltage fluctuates due to the variation in the load connected to the microgrid as the EV battery slowly discharges the DC bus voltage is brought to a predefined value of 600V and it is maintained there, henceforth by the battery discharge.

## V. Conclusion

The paper describes a PV-based smart EV charging system that allows for bidirectional power transfer. The voltage of the common DC connection, the EV battery SOC, and the present loading circumstances determine the charging system's mode of operation. The charging speed may also be adjusted based on the dampening level. The utilization of electric vehicles as the energy storage medium is the most crucial feature of this charging method. The diversity factor of the power system may be considerably increased by having efficient control over the EV load schedule. This may be accomplished by enlisting the help of EV owners in this two-way power flow arrangement. The utilization of EVs as energy storage devices and the usage of PV-based microgrid linked EV charging is an exciting technology that can help popularise EVs.

## Acknowledgment

The authors would like to thank SERB, DST, Govt. of India for supporting the research vide no. IMRC/AISTDF/CRD/2018/000013.



Authorized licensed use limited to: NATIONAL INSTITUTE OF TECHNOLOGY ROURKELA. Downloaded on April 16,2023 at 12:24:07 UTC from IEEE Xplore. Restrictions apply.

## References


[1] P. Goli and W. Shireen, "PV integrated smart charging of EVs based on DC link voltage sensing", *IEEE Transactions on Smart Grid*, vol. 5, no. 3, pp. 1421-1428, 2014.

[2] I. Bertini, D. A. Sbordone, M. C. Falvo, B. Di Pietra, L. Martirano, and A. Genovese, "EV fast-charging stations and energy storage technologies: a real implementation in the smart microgrid paradigm", *Electrical Power Systems Research*, vol. 120, pp. 96-108, 2015.

[3] J. Han, X. Zhou, S. Lu, and P. Zhao, "A three-phase bidirectional grid-connected AC/DC converter for V2G applications", *Journal of Control Science and Engineering*, vol. 2020, p. 12, 2020.

[4] S. Thangaprakash and S. M. Murugappan, Advances in Electrical and Computer Technologies. Springer Links, 2013.

[5] M. Rashid, Power electronics. Pearson, 2009.

[6] M. S. Vasisht, "Project thesis on design and development of solar-assisted power supply system for multi-services in railways", submitted to VTU, Belgaum, 2011.

[7] D. Freeman, "Introduction to photovoltaic systems maximum power point tracking. application report", *Texas Instruments*, no. SLVA446, 2010.

[8] J. Lowry, J. Larminie, O. Brookes, C. Engineer, and Swindon, Electric vehicle technology explained, 2nd ed. Oxford: Wiley, John & Sons, 2012.

[9] Kirkham, H. Current Measurement Methods for the Smart Grid. In Proceedings of the Power & Energy Society General Meeting, Calgary, AB, Canada, 26–30 July 2009.

[10] Azhar Ul-Haq, Carlo Cecati, Essal A. Al-Ammar, "Modeling of a Photovoltaic-Powered Electric Vehicle Charging Station with Vehicle to Grid Implementation", *Energies*, MDPI, 2017.

[11] Md Apel Mahmud, Tushar Kanti Roy, Shama Naz Islam, Sajeeb Saha, Md Enamul Haque. "Nonlinear Decentralized Feedback Linearizing Controller Design for Islanded DC Microgrids*", Electric Power Components and Systems*, 2018.

[12] Vishal Dabra, Krishan Kumar Paliwal, Pardeep Sharma, Narender Kumar. "Optimization of photovoltaic power system: a comparative study", *Protection and Control of Modern Power Systems*, 2017.

[13] Colm J. O'Rourke, Mohammad M. Qasim, Matthew R. Overlin, James L. Kirtley. "A Geometric Interpretation of Reference Frames and Transformations: dq0, Clarke, and Park*", IEEE Transactions on Energy Conversion*, 2019.

[14] Adama Ouedraogo, Serge Dimitri Y. B. Bazyomo, Salifou Ouedraogo, Abdoul Razakou, Dieudonné Joseph Bathiebo. "Improvement of the Silicon Solar Cell Performance by Integration of an Electric Field Source in the Solar Cell or Solar Module System", *Smart Grid and Renewable Energy*, 2018.

[15] Natarajan, "Capacitors for Miscellaneous Applications", Power Engineering (Willis), 2005.

[16] Xuhui, Zhang, Xuhui Wen, Zhao Feng, and Guo Xinhua. "A new control strategy for bi-directional DC-DC converter in electric vehicle", *2011 International Conference on Electrical Machines and Systems*, 2011.

[17] Duncan, Stafin L, "A Microgrid Design for DC Bus Voltage Stability and Improved Power Quality.", Lamar University - Beaumont, 2020.

[18] S.Y. Hui, Henry Shu-Hung Chung, Siu-Chung Yip. "A bidirectional AC-DC power converter with power factor correction", *IEEE Transactions on Power Electronics*, 2000.




Authorized licensed use limited to: NATIONAL INSTITUTE OF TECHNOLOGY ROURKELA. Downloaded on April 16,2023 at 12:24:07 UTC from IEEE Xplore. Restrictions apply.

# 2.ICSGTEIS-2021_pravat

ORIGINALITY REPORT

| 11% | 0% | 11% | 0% |
| --- | --- | --- | --- |
| SIMILARITY INDEX | INTERNET SOURCES | PUBLICATIONS | STUDENT PAPERS |

MATCH ALL SOURCES (ONLY SELECTED SOURCE PRINTED)

13%

★ Anindya Bharatee, Pravat Kumar Ray, Pratap Sekhar Puhan. "Power Management in a PV Integrated Electric Vehicle Charging System", 2022 IEEE Global Conference on Computing, Power and Communication Technologies (GlobConPT), 2022

Publication

| | | | |
| --- | --- | --- | --- |
| Exclude quotes | On | Exclude matches | < 10% |
| Exclude bibliography | On | | |

# 2.ICSGTEIS-2021_pravat

GRADEMARK REPORT

FINAL GRADE

/0

GENERAL COMMENTS

**Instructor**

PAGE 1

PAGE 2

PAGE 3

PAGE 4

PAGE 5

PAGE 6